

Observing and interpreting the seasonal variability of the oceanographic fluxes passing through Lancaster Sound of the Canadian Arctic Archipelago

Simon Prinsenber, Jim Hamilton, Ingrid Peterson and Roger Pettipas

Department of Fisheries and Oceans Canada, 1 Challenger Drive, Bedford Institute of Oceanography, P.O. Box 1006, Dartmouth, Nova Scotia, Canada, B2Y 4A2
PrinsenberS@mar.dfo-mpo.gc.ca

Abstract As part of the Arctic/Sub-Arctic Ocean Flux (ASOF) and the International Polar Year (IPY) programs, a research project consisting of mooring and analysis work has studied the ocean and ice fluxes passing through Lancaster Sound, one of the three main pathways through the Canadian Arctic Archipelago (CAA) since 1998. The aim is to understand the variability in ocean and sea ice volume, heat and freshwater fluxes passing through the CAA and to determine their relationship to the ocean and ice budgets of the Arctic Ocean itself and to the circulation and vertical ventilation of the North Atlantic Ocean. Eight years of mooring data have now been processed and analyzed. The volume, freshwater and heat fluxes exhibit large seasonal and interannual variabilities with small fluxes in the fall and early winter and large fluxes in the summer. The seasonal mean volume flux estimates range from a low of 0.0Sv in the fall of 1998 to a maximum of 1.3Sv in the summer of 2000 ($1\text{Sv} = 1.0 \times 10^6 \text{m}^3 \text{s}^{-1}$). It has an 8yr annual mean of 0.7Sv and varies interannually by $\pm 0.3\text{Sv}$. Model simulations indicate that fluxes through Lancaster Sound make up 40-50% of the fluxes through the entire Canadian Arctic Archipelago, and that they are dependent on the sea level difference between the Beaufort Sea and Baffin Bay and on the horizontal density gradients across the CAA, observations of which are scarce or non-existent. Regression analysis with the Arctic Ocean wind field shows that the fluxes through the NW Passage measured in Lancaster Sound are significantly correlated with the far field wind forcing in the Beaufort Sea. The northeastward winds in the Beaufort Sea, parallel to the western side of the Canadian Arctic Archipelago, show the highest correlation on monthly to interannual time scales. This result is consistent with the transport being driven by a sea level difference between opposite ends of the NW Passage, and the difference being determined by setup caused by along-shore winds in the Beaufort Sea.

INTRODUCTION

It is generally accepted now that due to climate change, the polar ice caps are melting (ACIA 2004, 2005 and IPCC 2007) and indeed, the Arctic Ocean ice extent of September 2007 was the smallest observed over the past 30 years, when satellite imagery was available to document accurately its extent (National Snow and Ice Data Centre, www://nsidc.org). In addition, all three NW Passage routes through the Canadian Arctic Archipelago (CAA) were ice free for the first time over the 30yr satellite observation period. Changes in the oceanographic and ice fluxes due to natural variability and due to climate change within the CAA have been monitored since August 1998 in Lancaster Sound as part of the international Arctic/Subarctic Ocean Flux (ASOF) program (ASOF 2004), and are being continued under the International Polar Year. The moorings have been monitoring the volume, heat and freshwater fluxes passing through Barrow Strait, the southernmost passage of three within the CAA connecting the Atlantic with the Arctic Ocean. The aim of the program is to better understand the oceanographic and pack ice fluxes passing through the Archipelago, their interannual variability and their relationship to the heat and freshwater budgets of the Arctic Ocean and the CAA, and to the circulation and vertical ventilation of the North Atlantic Ocean.

The first three years of processed data from the Lancaster Sound mooring project were reported in Prinsenbergh and Hamilton (2005), which described the instrumentation and high frequency variability in ocean parameters. Annual mean transport in Lancaster Sound over 3 years (1998-2001) was found to vary by $\pm 0.25\text{Sv}$ about a mean of 0.75Sv , with seasonal fluxes being lowest in the fall and highest in the summer. Further results were published in Melling et al. (2008), describing the long-term variability seen in 6 years of processed data. Now 8 years of data are available to investigate the factors controlling the transport variability that up to now were not well understood. Past analysis of the 1981-82 data from Barrow Strait had shown that seasonal variations in sea level differences along the Northwest Passage are correlated with seasonal variations in transport (Prinsenbergh and Bennett 1987); but these results were not connected to the atmospheric forcing. Analyses now indicate that sea level along the coasts of the Arctic Ocean is lower in winter (December-May) than in summer (June-November) because of Ekman transport away from the coasts associated with winter anticyclonic atmospheric circulation (Proshutinsky and Johnson 1997). The present analysis will show the relationship between winds on monthly to interannual time scales and the flow through Lancaster Sound, using transport estimates from 8 years of mooring data (1998-2006).

MOORING INSTRUMENTATION

Lancaster Sound is 65km wide at the mooring site and reaches depths of 285m

(Fig. 1). Annually the mooring array has been recovered and re-deployed in late summer using Canadian Coast Guard icebreakers, at which time CTD profiles and water samples for chemical tracer analysis have been collected. Instrumentation of the array has increased through the years as additional instrumentation became available (Prinsenber and Hamilton 2005). Mobile and land-fast pack ice conditions are found normally for 10 months of the year. Ice ridge keels within the pack ice are a threat to moorings which, for this reason, were designed not to extend into the top 25m of the water column. Instrumentation includes Acoustic Doppler Current Profilers (ADCPs) to monitor ocean and ice velocities, Upward Looking Sonars (ULSs) to monitor ice drafts, and CTD units (MicroCats) to monitor water column properties at various depths. Fig. 2 shows the array used for the 2003-2004 deployment, which also included Tide Gauges and a CTD profiler called ICYCLER. Further descriptions of the instrumentation, data analysis and high frequency ocean variability can be found in Prinsenber and Hamilton (2005).

OCEAN PARAMETERS

Salinity and temperature profiles, collected during the summer mooring surveys show that the coldest water (-1.7°C) in summer is found at mid-depth. It has a salinity of 32.8-33.0 and represents water mass remnants of the winter surface mixed layer (Prinsenber and Hamilton 2005). Above this water mass lies a very stable surface layer formed by dilution by ice melt and local runoff and warming by the atmospheric heat flux. The warmest and freshest water is organized into buoyancy boundary currents that flow in opposite directions along the northern and southern shores. Below the cold mid-depth water mass, the water temperature and salinity increases with depth. This warmer deep water enters the area from northern Baffin Bay. Geostrophic current fields derived from density distributions shows an eastward flowing current that decreases with depth and extends from the southern shore of Lancaster Sound to 2/3 of the way across the Sound. A depth-varying current along the northern shore appears to be restricted to 1/3 of the northern part of the Sound and does not appear to contribute to the total flux through the cross-section.

Figure 3 shows a 2-month example of the current variability seen in Lancaster Sound. The 2-month data sections are bi-hourly along-shore currents at 10m depth from the southern and northern sites. These small sections of the total 8yr record show the temporal variability that exists throughout the 8yr time series. Ocean currents vary hourly due to tidal components, vary daily due to atmospheric forcing and vary seasonally due to long-term variability in sea level pressure gradients. In addition to these temporal variabilities at each location, there exist large horizontal and vertical spatial variabilities. Tidal currents vary on a 12hr cycle by up to 35cm/sec when the sun and moon tidal constituents generated in the Atlantic Ocean reinforce or oppose each other. The contribution from the Arctic Ocean tide is weaker as the Arctic tides are smaller and reflected back to the Arctic from the

sill and island arch located in western Barrow Strait at 96deg W longitude.

The largest long-term mean velocity components, driven by atmospheric and sea level pressure gradients along the NW Passage, are found along the southern shore where daily mean values of the exiting Arctic surface waters reach 50cm/sec and set towards Baffin Bay. Along the northern shore, the long-term currents are smaller and do not have a persistent preferred direction (Fig. 4). In the summer they generally are directed towards the west (Arctic Ocean) and in the winter towards the east (Baffin Bay). Currents normally decrease with depth in response to surface atmospheric forcing and bottom friction. The exception being that during land-fast ice conditions, the ice isolates the ocean surface from wind forcing and acts as a friction boundary thereby reducing the surface currents in winter relative to mid-depth values (Fig. 4). The seasonal and yearly mean currents vary interannually in response to large scale atmospheric forcing and as seen later to the sea surface level set-up due to surface winds at the western entrance of the NW Passage section in the CAA (Peterson 2008).

Figs. 5 and 6 show the bi-monthly ocean along-shore current data for the 8yr period. The bi-monthly mean velocities (solid dots) and magnitude of the standard deviation about the mean show that at both sites, the mean currents are lower and are less variable during the winter months than the summer months, when far-field and local wind forcing on the ocean surface can occur. In the summer months the mean currents and variability about the means are larger for the southern site and are setting eastwards to Baffin Bay. For the northern site, the summer means are small but generally setting to the west. The maximum velocities are similarly largest for the southern site, occur during the open water period and are in the direction of Baffin Bay. The maximum velocities towards the west are less as they oppose the mean currents flowing to Baffin Bay. In contrast, the largest summer maximum velocities along the northern shore are part of the buoyancy coastal currents directed towards the west.

ICE VELOCITIES, DRAFTS and FLUXES

The ADCPs providing ocean velocities, also provide ice drifts at bi-hourly intervals. To show the total 8yr time series, the bi-hourly ice velocity data were again divided into two-month sections for which the along-strait ice velocity was used to derive the bi-monthly vector mean velocities and the standard deviations (Std). Since ice is not always present in the summer months, the bi-monthly percent of ice velocity values was also calculated and shown in Figs. 7 and 8 for the southern and northern sites respectively.

Fig. 7 shows the results from the southern site of Lancaster Sound where most of the eastwards flowing Arctic surface waters occur (Prinsenbergh and Hamilton 2005). Land-fast ice conditions occur normally in March and April and in some

severe winters during the months of May and June. In 2003, the ice was mobile for at least part of each 2 month period and land-fast ice conditions did not occur for the total two month period (March-April). During mobile ice conditions, the bi-monthly mean velocities are up to 50cm/sec but are generally around 10cm/sec. In these periods, the percentage of ice present is low, allowing the ice to move freely under ocean and wind forcing. Ice velocities towards Baffin Bay are generally larger than those towards the Arctic, as they move along with the eastward bi-monthly mean ocean currents.

At the northern site, land-fast ice conditions persisted for the months of March and April for all years except 2003 and 2004 (Fig. 8). Bi-monthly vector mean ice velocities are smaller along the northern shore, and unlike at the southern site, have no preferred direction. In summer months the percentage of ice present drops below 25%, as was the case for the southern site.

Fig. 9 shows two years of ice draft data from the ice season of 2003-04 when the pack ice remained mobile throughout the winter, and from the ice season 2005-06 when land-fast ice conditions occurred and thus reflect a more normal ice season. With global warming however, mobile ice conditions such as those of 2003-04 may become more prevalent. During mobile ice conditions, ice ridges passing the mooring site reach up to 24m, but were generally up to 16m for the 2003-04 winter. In 2005-06 the maximum ice draft was 13m. From ice charts, it can be seen that the ice arch separating land-fast ice from mobile ice occurred in western Barrow Strait in 2003-04 (95deg. West), 120km west of the mooring site, while it established itself at the mooring site in the 2005-06 winter (Can. Ice Service, <http://ice-glace.ec.ca>). Once land-fast ice conditions were established at the mooring site in February 2006, the sonar monitored the same ice that grew slowly thermodynamically. For the 2005-06 winter, the land-fast ice above the sonar was not ridged and thus low monthly maxima were detected. The small variability detected in the monthly mean is probably due to mooring motion that causes the sonar to monitor ice in a small area and not just one specific location of the pack ice.

In the bottom panel of Fig. 9, the monthly mean draft and the standard deviation are shown for the 2003-04 and 2005-06 winters. Relative to the 2003-04 winter, the 2005-06 winter started and ended two months later. During mobile ice conditions the monthly Std of ice draft and the monthly mean ice draft vary similarly; meaning that the variability about the mean and the mean itself increase and decrease proportionally. During land-fast ice conditions the Std approaches zero and the mean values vary as expected under thermodynamic ice growth. Once the land-fast ice breaks up in June 2006, ridges start to appear and increase the monthly maximum.

To estimate the freshwater flux associated with the mobile pack ice requires ice drift and ice thickness data such as shown in Figs. 6, 7 and 8. However, not only are these time series scarce, but also very site-specific, as ice properties are less diffusive than ocean properties.

Although satellite imagery alone cannot provide estimates of ice-volume fluxes, it has provided long time series of ice-area fluxes in the CAA. However, the flux estimates are often hampered by coarse spatial resolution. Kwok (2006) estimated the ice-area transport across the main entrances to the Canadian Archipelago using Radarsat imagery (0.2km resolution) and found that due to the land-fast ice within the CAA, the western entrances export ice to the Arctic Ocean, and the eastern entrances export ice to Baffin Bay. On average, Nares Strait does export ice from the Arctic to Baffin Bay, but export is prevented when the ice bridge in Smith Sound is present. Agnew et al. (2006) using Advanced Microwave Scanning Radiometer AMSR-E data (6km resolution) found that transport directions were generally similar. However transport estimates differed in magnitude, perhaps because of different resolutions of the imagery or different time periods. In deriving ice-volume fluxes from ice-area fluxes for freshwater budgets, the uncertainty is further increased by the difficulty of estimating ice thickness. Freshwater fluxes in the form of ice that have been estimated from ADCP ice drift data (Prinsenber and Hamilton 2005; Melling et al. 2008) are in the range of 1.5-2.5mSv, and are an order of magnitude smaller than those in the water column.

OCEAN FLUXES

To estimate fluxes from site-specific time series it is assumed that the mooring data can represent, through weighting, the cross-sectional fluxes. Analysis of data from August 2001 to August 2004 of a modified array provided surface layer (0-60m) current measurements from $\frac{1}{4}$ and $\frac{1}{2}$ way across the strait as well as measurements at the southern and northern sites. These data indicate that in winter and spring, the eastwards currents are similar across the southern $\frac{2}{3}$ of the strait, while in summer and fall the currents of the southern mooring should be reduced to 55% to represent the mean currents observed over $\frac{2}{3}$ of the southern strait. This provides information to better estimate the total fluxes through the cross-section for the sparser arrays prior to 2001. Further details on the estimation of fluxes can be found in Prinsenber and Hamilton (2005) and Melling et al. (2008).

Fluxes are calculated relative to a salinity of 34.8 and a temperature of -0.1°C , which represents the salinity and temperature of Atlantic Water in the Arctic Ocean (Aagaard and Carmack 1989). Fluxes clearly show the strong seasonal as well as the interannual variability (Fig. 10). Volume and fresh water fluxes exhibit the same variability driven by the currents, while the heat flux mirrors their variability. All three show maximum magnitudes in the summer and minimum magnitudes in the fall. Volume and freshwater fluxes are positive indicating net transport of Arctic surface waters to the Atlantic Ocean. Heat flux is predominantly negative, indicating that Arctic surface water is colder than Atlantic Water in the Arctic Ocean, and will thus cool the Atlantic Ocean. It has an 8-yr mean of -4.1×10^5 Watts and varies interannually by $\pm 2.0 \times 10^5$ Watts. Seasonal (3-month aver-

ages) volume fluxes vary from low values in fall (0.0Sv in 1998) to high values in summer (1.3Sv in 2000). Annual means of the volume fluxes vary from 0.4 to 1.0Sv, and have an 8-yr mean of 0.7Sv. In general, the freshwater flux is 1/15 of the volume flux and follows the volume seasonal variability. It has an 8-yr mean of 0.048Sv and varies interannually by ± 0.015 Sv. The 8-yr flux data was used to derive the annual cycle, consisting of mean monthly values (Fig. 11). It has a maximum in June of 1.15Sv and a minimum in December of 0.25Sv.

WIND FORCING

The volume transport data were compared with NCEP (National Centre for Atmospheric Prediction) monthly surface wind data (sigma level=0.995), which has a grid spacing of 2.5° latitude by 2.5° longitude (Peterson 2008). Multiple correlation coefficients with the observed transports were computed using monthly mean wind data at each grid point (i,j) north of 55°N, and a regression model of the form

$$M = a_{ij}U_{ij} + b_{ij}V_{ij} + c_{ij} + \varepsilon \quad (1)$$

where M is volume transport, U_{ij} is the zonal wind component, V_{ij} is the meridional wind component at grid point (i,j), a_{ij} , b_{ij} , and c_{ij} are the regression coefficients, and ε is the residual.

The maximum correlation coefficient ($R=0.68$) is found in the Beaufort Sea west of M'Clure Strait at 75°N, 132.5°W, the western entrance of the NW Passage of the CAA. It is over 1000km from the mooring array in Lancaster Sound and its correlation coefficient is double that of the local wind forcing. The optimum wind direction at the western entrance to the NW Passage (thin arrow, Fig. 12) is to the northeast (43°T), which is parallel to the coastline. Similarly, an optimum wind direction parallel to the western Newfoundland coastline was reported for flow in the Strait of Belle Isle (Garrett and Toulany 1981), and was explained by the winds causing sea level setup or setdown at the ends of the strait, producing a sea level difference from one end to the other.

However, the location of the maximum correlation is not well defined. Since some portion of the correlation may be simply due to the wind and transport having similar annual cycles, the analysis was repeated using monthly anomalies of transport and wind components, computed by subtracting the 8-yr mean values for each month. For this second case, the correlation coefficient reduced slightly from 0.68 to 0.62 and remained off the western entrance of the Northwest Passage (thick arrow in Fig. 12). The optimum direction is toward 44°T, and the time series for the wind anomaly component along this direction is plotted in Fig. 13. The gains, monthly wind anomalies, and the mean annual cycle of transport were used to produce estimates of transport (Fig.13). The annual cycle of transport represents 34% of the variance of total transport, and the wind anomalies combined with the

annual cycle account for 59% of the variance of monthly transport.

The regression coefficients can be used to simulate the transport through Lancaster Sound for other years prior to 1998. Fig. 14 shows the monthly simulated transports back to 1980 when the first transport observations were available from Barrow Strait just west of the present mooring array site (Prinsenber and Bennett, 1987). The observations compare well with the wind estimates; they are smaller at this site because some of the transport flux coming out of the Sverdrup Basin east of Cornwallis Island (Fig. 1) is not included, as it is in the present mooring observations. Assuming that Barrow Strait contributes three-quarters of the transport of Lancaster Sound (Prinsenber and Bennett, 1987), the 1981-1982 observations should be increased by one-third.

The annual mean transport (August to July) from 1999 to 2006 (Fig.15) is also significantly correlated with the alongshore wind ($r=0.88$) based on 8 points (years). The gain is $0.24 \times 10^6 \text{ m}^2$, and using the relationship between annual mean transport and wind (1999-2006), transport was estimated for the full extent of the NCEP dataset (Fig. 15). The lowest estimated transport value over the entire 58-year record corresponded to the year 1999, while 2001 had the fourth highest value. The extreme low was captured in our mooring observation period. Estimated transport was particularly high from 1989 to 1997, and may have contributed to the freshwater gain observed in the Labrador Sea during this period (Yashayaev 2007).

The Arctic Oscillation index, defined as the leading principal component of Northern Hemisphere SLP, is plotted in Fig. 15, and is averaged between August and July as for the transport estimates based on the alongshore wind. At any given point, the correlation between the along-shore wind component and the AO index is expected to depend on the loading pattern of the AO index. The correlation of alongshore wind at 75°N , 125°W with the AO index is 0.60. Not surprisingly, the AO and the alongshore wind show similar trends and inter-decadal variability, with high values seen in the early 1990's. However the AO does not capture the interannual variability of the observed transport over the 8-yr mooring deployment ($r=0.21$).

CONCLUSION

Due to the eastward-setting Arctic surface waters found along the southern shore of Lancaster Sound, the mean currents there are large (15.3cm/sec) as compared to smaller westward-setting mean currents of 2.2cm/sec along the northern shore. Standard deviations about the 8yr mean are 21.5 and 15.0cm/sec respectively for the southern and northern shore sites, while maximum values can reach up to 150cm/sec. Bi-monthly mean velocities reach up to 50cm/sec in summer months along the southern shore, while they only reach 10cm/sec along the northern

shore.

Bi-monthly mean ice drifts are smaller because of the long period of land-fast ice conditions, but can similarly reach maximum speeds of 150cm/sec. Ice draft measurements were available for only two years and show that the mean, standard deviation and maximum keel depth depend on whether landfast ice occurs at the mooring site. Ice volume fluxes and derived freshwater fluxes in the form as ice are difficult to estimate but appear to be an order of magnitude less than the freshwater fluxes in the water column.

Volume, freshwater and heat transports estimated from the mooring data clearly show the strong seasonal as well as the interannual variability. Heat fluxes are predominantly negative indicating that the Arctic surface water is colder and will cool the Atlantic Ocean. Yearly means of the volume fluxes vary from 0.4 to 1.0Sv, and have an 8-yr mean of 0.7Sv. In general, the freshwater flux is 1/15 of the volume flux and follows the volume seasonal variability. It has an 8-yr mean of 0.048Sv and varies interannually by ± 0.015 Sv.

The 8-yr mean monthly volume flux has a summer maximum (1.15Sv) and a late-fall minimum (0.25Sv). Seasonal mean values are as low as -0.01Sv for fall and as high as 1.32Sv for summer.

Volume transport in Lancaster Sound is significantly correlated with northeastward winds in the Beaufort Sea, parallel to the western side of the CAA, at monthly to interannual time scales. The optimum location and wind direction are consistent with the flow being driven by a sea level difference along the Northwest Passage, and the difference being determined by setup caused by alongshore winds in the Beaufort Sea.

Freshwater and heat transport are highly correlated with volume transport. The correlation coefficients between volume transport and freshwater and heat transport are greater than 0.96 for both total transport and transport anomalies. Thus based on the transport estimates, the results for volume transport generally apply for freshwater and heat transport as well. However, freshwater transport is likely underestimated since it is based on measurements from Conductivity-Temperature-Depth (CTD) sensors at depths greater than 25-30m (Prinsenber and Hamilton 2005).

Wind forcing is also important in determining transport in Bering Strait at both weekly to monthly time scales and interannual time scales (Woodgate et al. 2006). However, the transport is primarily affected by local winds parallel to the strait. The mean transport is northward, and is weakest in winter because of strong northerly winds, and strongest in summer.

In contrast, in Lancaster Sound, transport variability is largely determined by winds 1000km away at the western end of the Northwest Passage parallel to the

adjoining coasts. The mean transport is eastward, and transport is lowest in the fall because of strong northeasterly winds. Transport increases in January-February because of a high pressure ridge over the area producing a weaker northeasterly wind component. Highest transport is observed in the summer because of moderate westerly winds. The correlation of alongshore wind at 75°N, 125°W with the AO index is 0.60 as the alongshore wind show similar trends and inter-decadal variability. However the annual AO index does not capture the interannual variability of the observed transport over the 8-yr mooring deployment ($r=0.21$).

Acknowledgments

The authors would like to thank Murray Scotney for managing the instrumentation for the collection of all the mooring data. Internal and external reviewers are thanked for their helpful comments on the various drafts of the manuscript. Personnel of Canadian Coast Guard icebreakers are thanked for their continued support during field operations. This work was supported by the Canadian Program of Energy Research Development (PERD) and the Department of Fisheries and Oceans' High Priority Program.

REFERENCES

- Aagaard K, Carmack EC (1989) On the role of sea ice and freshwater in the Arctic circulation. *J Geophys Res* 94:14485-14498
- ACIA (2004) Impacts of a warming Arctic: Arctic Climate Impact Assessment. Cambridge University Press
- ACIA (2005) Arctic Climate Impact Assessment. Cambridge University Press
- Agnew TA, Vandewedge J, Lambe A (2006) Estimating the sea ice area flux across the Canadian Arctic Archipelago using the Advanced Microwave Scanning Radiometer (AMSR-E). Unpublished report
- ASOF (2004) Arctic/Subarctic Ocean Fluxes. Newsletter No2, March 2004 <http://asof.npolar.no>
- IPCC (2007) IPCC fourth Assessment report (AR-4). Twenty-Seventh Session of the International Panel on Climate Change, Valencia Spain, Nov 12-17, 2007
- Garrett CJR, Toulany B (1981) Variability of the flow through the Strait of Belle Isle. *J Mar Res* 39: 163-189
- Kwok R (2006) Exchange of sea ice between the Arctic Ocean and the Canadian Arctic Archipelago. *Geophys Res Lett* 33 L16501, doi:10.1029/2006GL027094. 1
- Melling M, Agnew TA, Falkner KE, Greenberg DA, Lee CM, Munchow A, Petrie B, Prinsenberg SJ, Samelson RM and Woodgate RA (2008) Fresh-water fluxes via

Pacific and Arctic outflows across Canadian Polar Shelf. In: Dickson RR, Meinke J and Rhines P (ed) *Arctic-Subarctic Ocean Fluxes, Defining the role of the northern seas in climate*, Springer Science and Business Media BV

Peterson IK (2008) Beaufort Sea wind forcing of the flow through the Northwest Passage. *Geophys Res Lett*, submitted

Prinsenberg SJ, Hamilton J (2005) Monitoring the volume, freshwater and heat fluxes passing through Lancaster Sound in the Canadian Arctic Archipelago. *Atmosphere-Ocean* 43(1): 1-23

Prinsenberg SJ, Bennett EB (1987) Mixing and transports in Barrow Strait, the central part of the Northwest Passage. *Cont Shelf Res* Vol 7(8): 913-935

Proshutinsky AY, Johnson MA (1997) Two circulation regimes of the wind driven Arctic Ocean. *J Geophys Res* 102:12493–12514

Woodgate RA, Aagaard K, Weingartner TJ (2006) Interannual changes in the Bering Strait fluxes of volume, heat and freshwater between 1991 and 2004. *Geophys Res Lett*, 33, L15609, doi:10.1029/2006GL026931

Yashayaev I (2007) Hydrographic changes in the Labrador Sea, 1960-2005. *Progress in Oceanography* 73:242-276

Figures

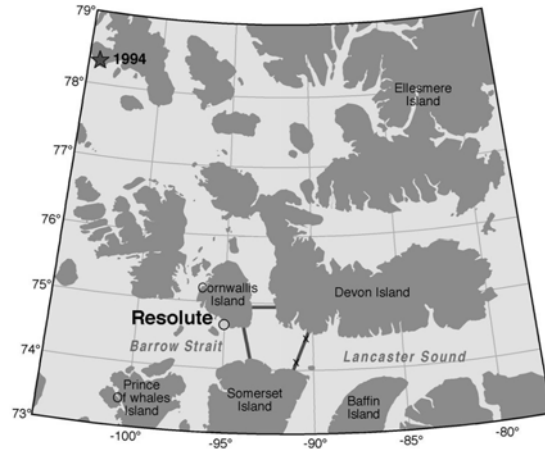


Fig. 1. Map of the eastern Canadian Arctic Archipelago (CAA) section of the NW Passage showing the CTD transects as solid lines, main mooring sites (crosses) in the Barrow Strait-Lancaster Sound region and the north magnetic pole location (Star-1994) which is moving northwards.

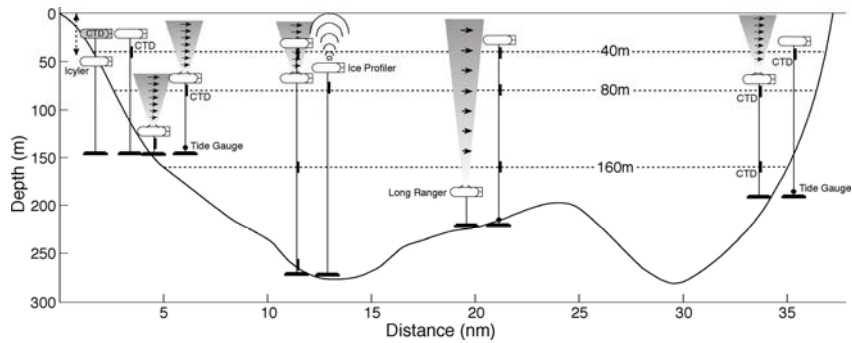


Fig. 2. Lancaster Sound mooring array for 2003-04 looking upstream to the Arctic Ocean with the south shore on the left of the figure and north on the right (37nm equals 65km).

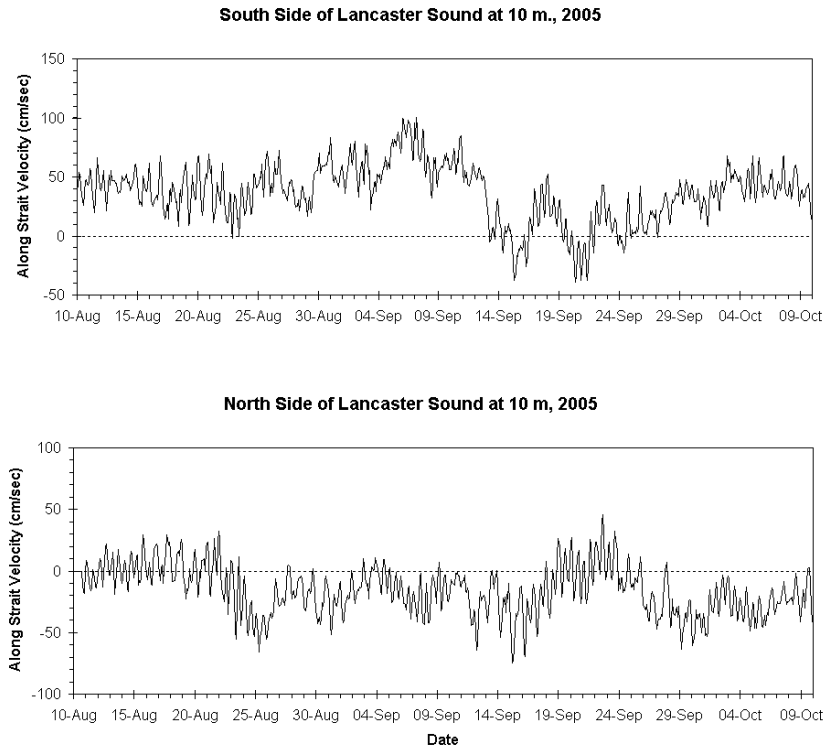


Fig. 3. Along-shore ocean surface velocities (10m depth) from the southern and northern mooring sites in Lancaster Sound. Bi-hourly data are from August 10 to October 9, 2005.

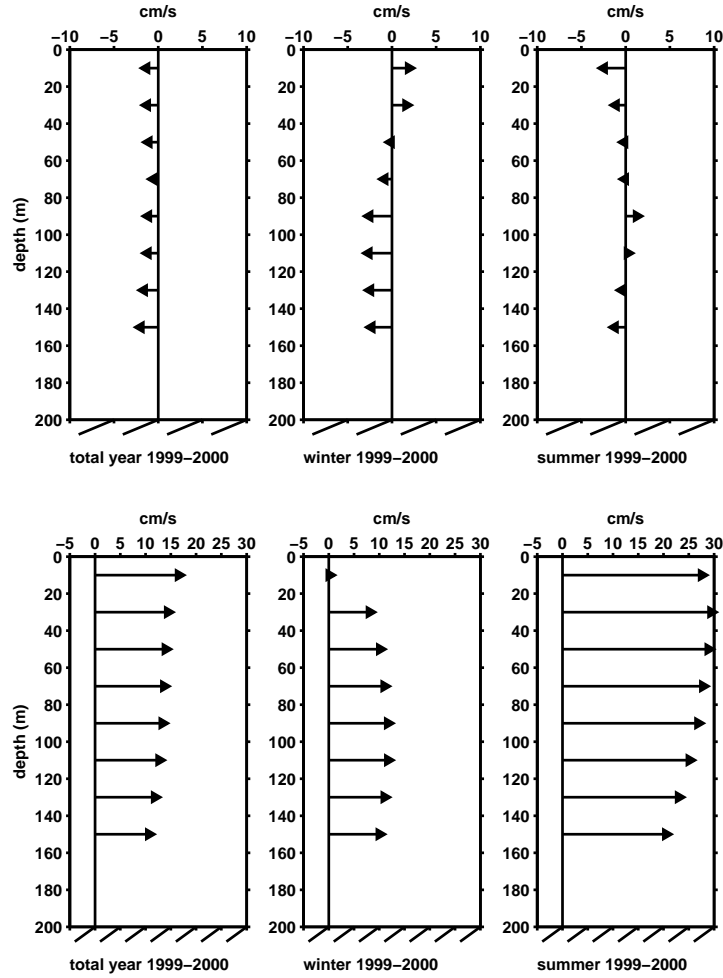


Fig. 4. Along-shore current profiles for the northern (top) and southern (bottom) sites in Lancaster Sound. Profiles are for year-long deployment of August 1999 to August 2000, the winter 2000 (January to April) and the summer 2000 (June to mid August).

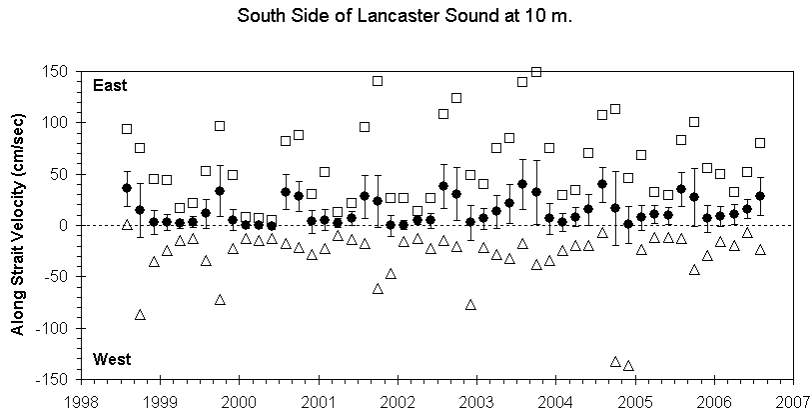


Fig. 5. Eight years of bi-monthly ocean velocity data observed at 10m depth at the southern site in Lancaster Sound. Shown are bi-monthly vector velocity means (solid circles), standard deviations (bars), and the maximum east (squares) and maximum west bi-hourly velocities (triangles) for each bi-monthly section.

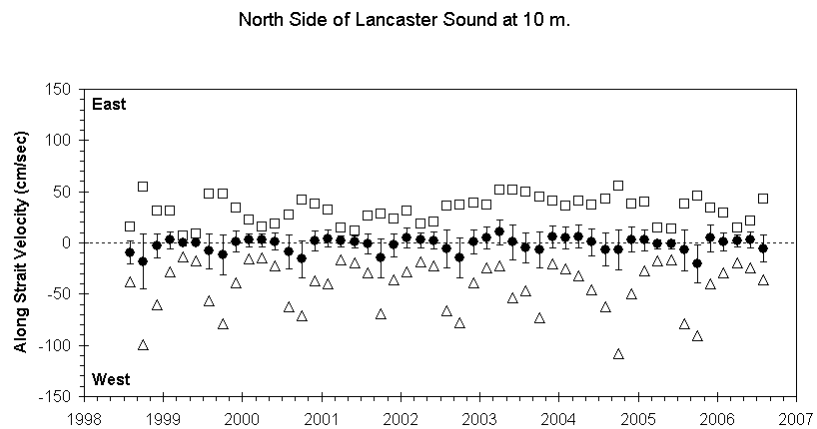


Fig. 6. Same as Fig. 5 but for the northern site in Lancaster Sound.

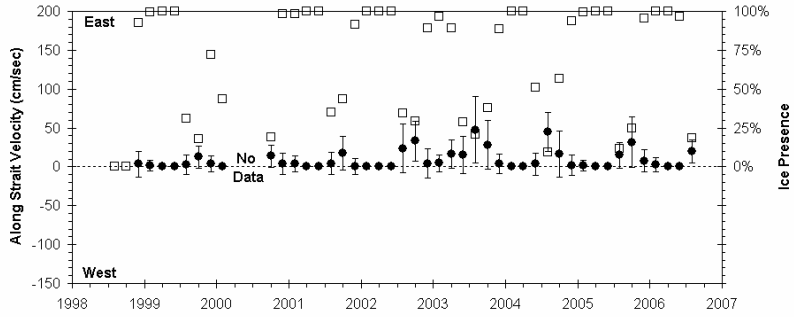


Fig. 7. Eight years of ice velocity data observed in Lancaster Sound located at a site 5nm from the southern shore (Fig. 2). Bi-monthly means are shown as solid circles, with ± 1 standard deviation illustrated with the bars. Percentage of ice presence providing ice velocities are shown by open squares.

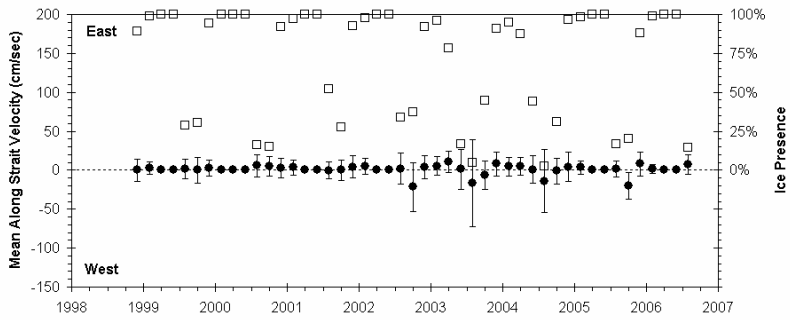


Fig. 8. Same as Fig. 7 but for site 3nm from the northern shore in Lancaster Sound (Fig. 7).

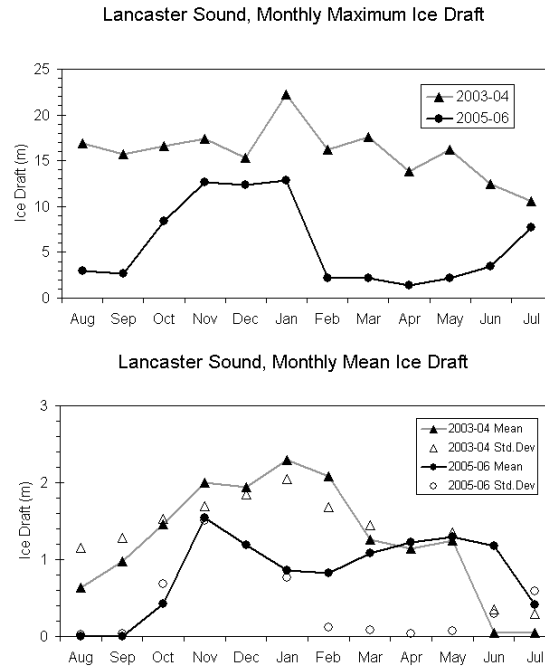


Fig. 9. Two years of ice draft data from the southern site of the Lancaster Sound array. Shown are monthly maxima ice draft (top panel) and monthly means and standard deviations in the bottom panel.

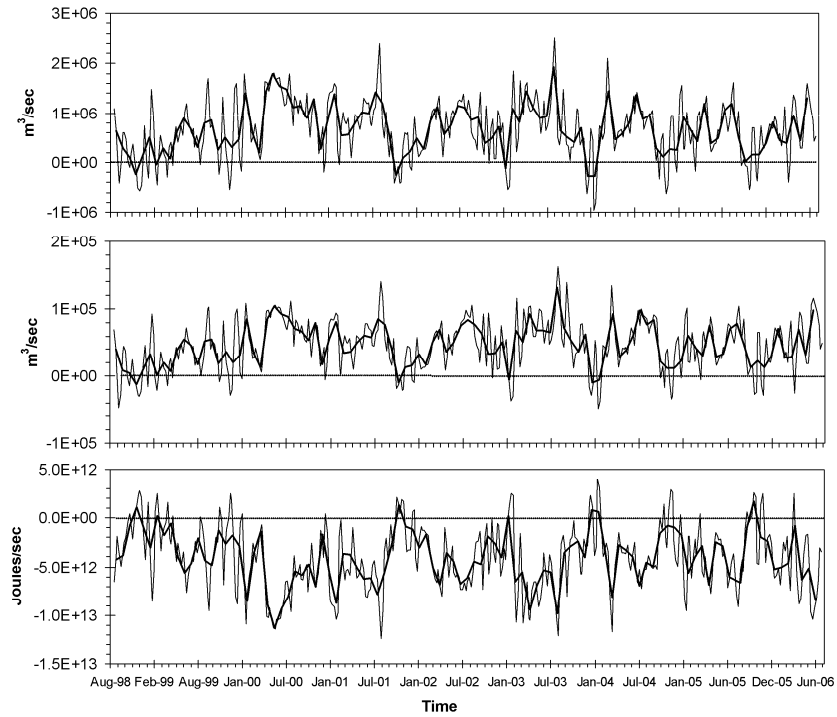


Fig. 10. Weekly (thin line) and monthly (thick line) estimated volume (top), freshwater (middle) and heat (bottom panel) transports through Lancaster Sound from August 1998 to August 2006.

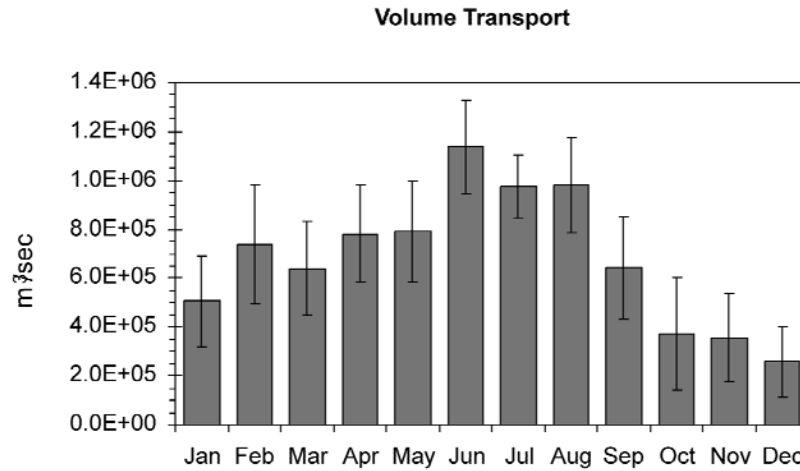


Fig. 11. Mean monthly volume flux through western Lancaster Sound derived from 8 years of mooring data (Aug. 1998 – Aug. 2006).

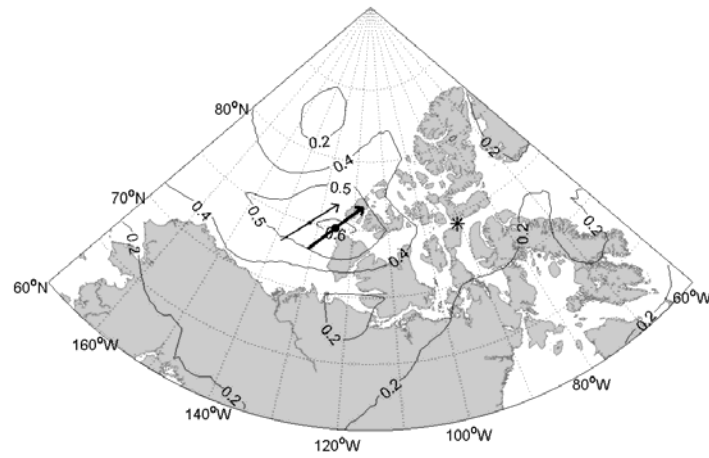


Fig. 12. Map showing correlation coefficients between monthly anomalies of NCEP surface wind and volume transport (contour lines), and the optimum wind location and direction (thick black arrow). The position of the Lancaster Sound mooring line is marked by the asterisk. The thin black arrow shows the optimum wind location and direction using monthly total wind and volume transport.

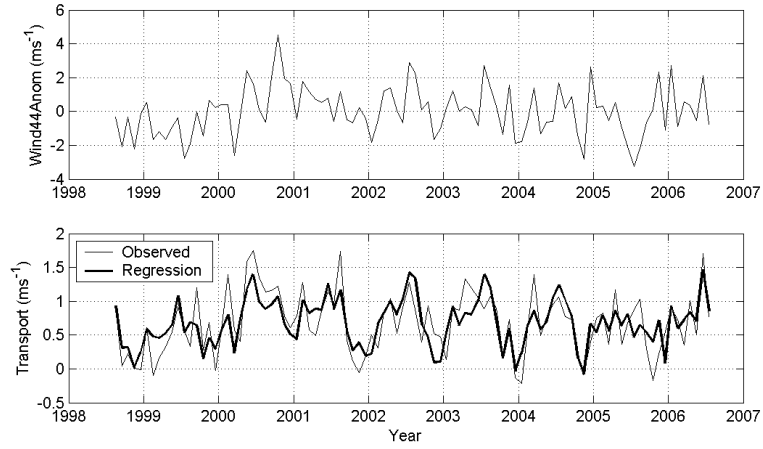


Fig. 13. Alongshore component of monthly wind anomalies at 75°N, 125.0°W (relative to 44°T) and annual cycle plus the wind anomaly effect (bold line), and the observed volume transport (thin line).

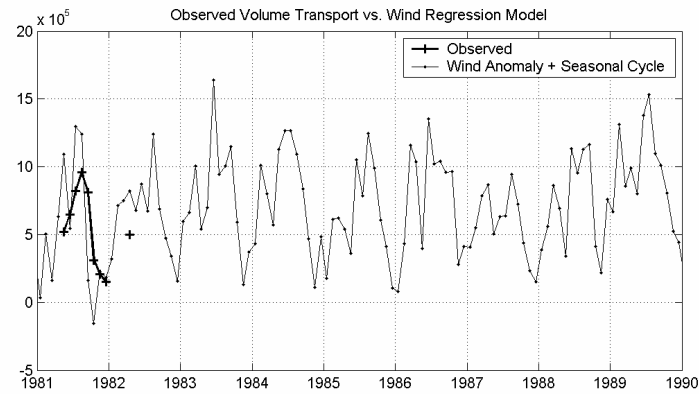


Fig. 14. Monthly transport estimates for the 1980's including the Barrow Strait observations (bold line) derived from the NCEP winds.

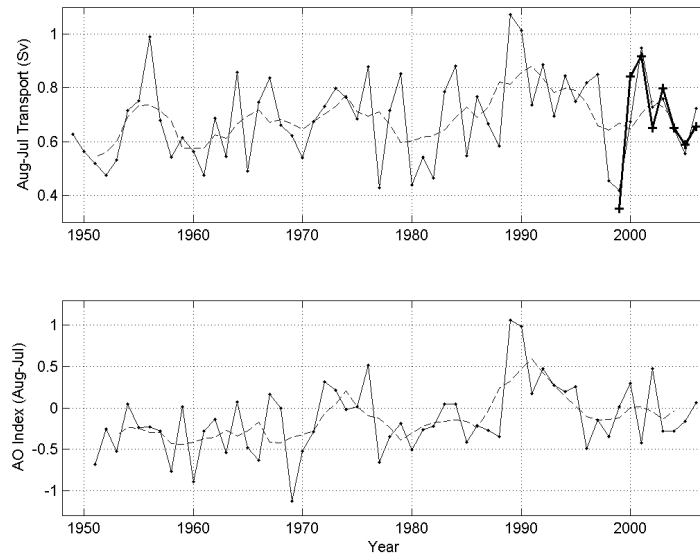


Fig. 15. Top panel shows annual mean transport (August-September) estimated from alongshore winds (thin solid line) and observed transport (bold line). Bottom panel shows the Arctic Oscillation (solid line). The 5-year running means are shown by the dashed lines in both panels.